

INERTANCE TUBE OPTIMIZATION FOR PULSE TUBE REFRIGERATORS*

Ray Radebaugh¹, M. Lewis¹, E. Luo²,
J. M. Pfothauer³, G. F. Nellis³, and L. A. Schunk³

¹National Institute of Standards and Technology
Boulder, Colorado, 80305, USA

²Technical Institute of Physics and Chemistry, CAS
Beijing, 100080, China

³University of Wisconsin-Madison
Madison, Wisconsin, 53706, USA

ABSTRACT

The efficiency of regenerative refrigerators is generally maximized when the pressure and flow are in phase near the midpoint of the regenerator. Such a phase relationship minimizes the amplitude of the mass flow for a given acoustic power flow through the regenerator. To achieve this phase relationship in a pulse tube refrigerator requires that the flow at the warm end of the pulse tube lag the pressure by about 60 degrees. The inertance tube allows for the flow to lag the pressure, but such a large phase shift is only possible with relatively large acoustic power flows. In small pulse tube cryocoolers the efficiency is improved by maximizing the phase shift in the inertance tube. This paper describes a simple transmission line model of the inertance tube, which is used to find the maximum phase shift and the corresponding diameter and length of the optimized inertance tube. Acoustic power flows between 1 and 100 W are considered in this study, though the model may be valid for larger systems as well. For large systems the model can be used to find the minimum reservoir volume that in combination with the inertance tube provides a phase shift of 60 degrees. This transmission line model is compared with some experimental results on a small-diameter inertance tube and found to agree quite well provided some heat transfer is taken into account. Design graphs for a frequency of 60 Hz and an average pressure of 2.5 MPa are presented for different pressure ratios and for both adiabatic and isothermal conditions.

* Contribution of NIST, not subject to copyright in the US.

INTRODUCTION

Flow in Regenerators

Most losses in pulse tube refrigerators occur in the regenerator. Significant losses also occur inside the pulse tube component if secondary flows, such as turbulence, acoustic streaming, and DC flows are not eliminated or minimized. The function of the regenerator is to transmit a given acoustic or PV power from the compressor to the cold end with a minimum of losses. These losses include thermal ineffectiveness, lost power associated with pressure drop, and axial thermal conduction. The first two scale directly with the amplitude of mass or volume flow through the regenerator. The time-averaged acoustic power transmitted through the regenerator is given by [1]

$$\langle \dot{W} \rangle_t = \langle P\dot{V} \rangle_t = (1/2)|P||\dot{V}| \cos \theta = (1/2)|P| \frac{|\dot{m}|}{\rho_0} \cos \theta = (1/2)RT_0 \frac{|P|}{P_0} |\dot{m}| \cos \theta, \quad (1)$$

where the bold symbols represent time-varying or phasor variables, such as pressure, volume flow rate, and mass flow rate. The phase angle θ is the phase between pressure and flow. The other symbols are: ρ_0 is the average density, R is the gas constant per unit mass, T_0 is the average temperature, and P_0 is the average pressure. The expression to the right of the first equal sign is the general expression, the expression to the right of the second equal sign applies to a harmonic approximation, the expression to the right of the third equal sign substitutes the mass flow for the volume flow, and the expression to the right of the fourth equal sign applies to an ideal gas. From equation (1) we see that the acoustic power flow is proportional to the component of the mass flow in phase with the pressure. Thus, minimizing the ratio of the regenerator losses to the acoustic power flow entails minimizing θ , the phase between flow and pressure. Because of the gas volume in the regenerator the conservation of mass requires that the flow at the warm end will necessarily lead the flow at the cold end. In that case the optimum phase relationship is that in which $\theta = 0$ at approximately the midpoint of the regenerator. Typically the flow at the cold end will lag the pressure by about 30° , whereas at the warm end the flow will lead the pressure by about 30° . Such a phase relationship is easily achieved in a Stirling refrigerator by selecting the appropriate displacer swept volume and phase. Figure 1 shows a phasor representation of mass conservation in a Stirling refrigerator that shows the optimum phase relationship of $\theta = 0$ at approximately the regenerator midpoint. In a pulse tube refrigerator with only an orifice or other resistive flow element for setting the phase, the flow will be in phase ($\theta = 0$) at the orifice, but not at the regenerator midpoint. Figure 2 shows the phasor representation of the orifice pulse tube refrigerator (OPTTR). In that case θ may be approximately 30° at the cold end, 50° or more at the midpoint, and as much as 70° at the warm end. With such a large phase angle the amplitude of mass flow required at the warm end of the regenerator for a given acoustic power flow will be more than twice that in which $\theta = 0$ at the midpoint of the regenerator. Such a high mass flow leads to a large regenerator ineffectiveness and pressure drop.

Regenerator and Pulse Tube Losses

Figure 3 shows how regenerator losses vary with the phase angle between the flow and the pressure for a given entropy flow at the warm end of the regenerator. Fixing the entropy flow there is similar to fixing the acoustic power flow at the warm end. The results

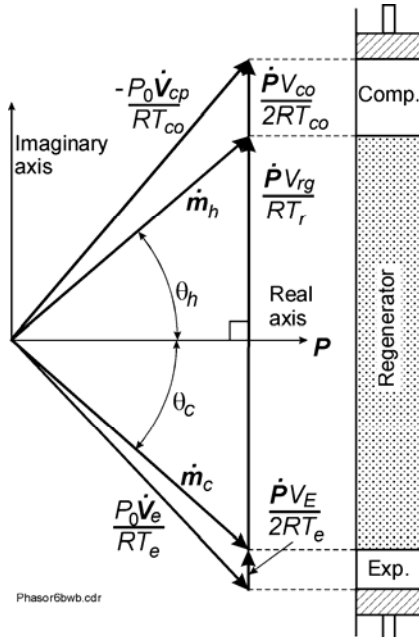


FIGURE 1. Phasor diagram of mass conservation in a Stirling refrigerator.

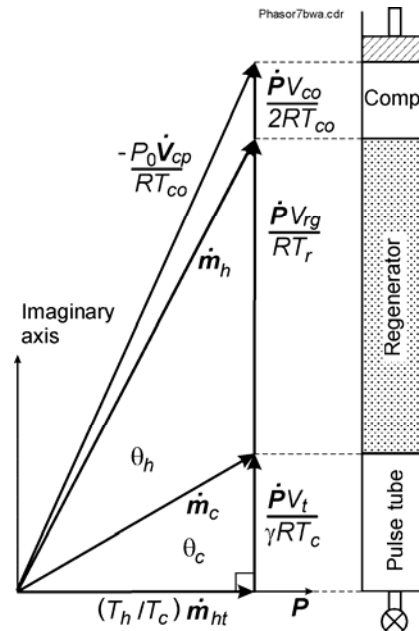


FIGURE 2. Phasor diagram for an orifice pulse tube refrigerator.

in this figure were calculated using the NIST numerical regenerator model known as REGEN3.2 [1]. This figure shows that the minimum regenerator loss occurs with the flow lagging the pressure at the cold end by about 30°, which typically is achieved with a Stirling refrigerator. With an OPTR the phase angle is about +30° (flow leading pressure) at the cold end. As this figure shows, the sum of the ineffectiveness loss \dot{S}_{reg} and the pressure drop loss $\dot{S}_{\Delta P}$ for the OPTR is about twice that for the optimum phase of about -30° at the cold end. The addition of a secondary orifice in the double inlet pulse tube refrigerator (DIPTR) [2] permits shifting the phase at the cold end to about 0° without a large additional loss in the secondary orifice. As Fig. 3 shows, the DIPTR then has a smaller total regenerator loss than the OPTR. However the DIPTR has the disadvantage

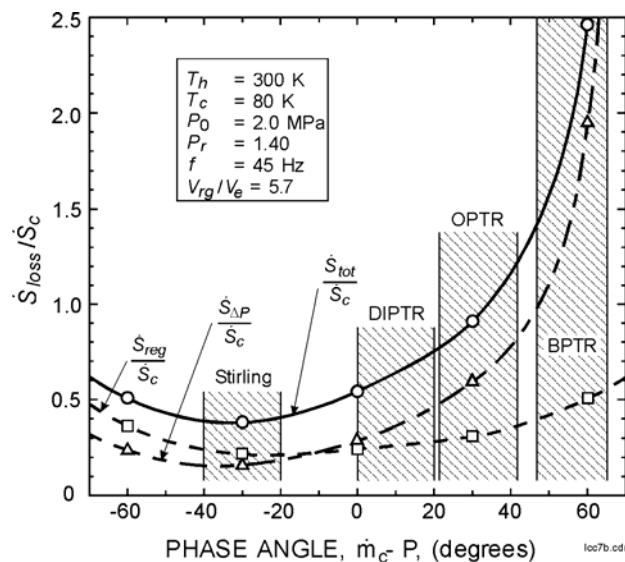


FIGURE 3. Regenerator losses associated with ineffectiveness and pressure drop for various phase angles by which flow leads pressure. Results from calculations with REGEN3.2 [1].

that it opens up a continuous flow loop that allows a DC flow to occur with an accompanying loss and instability that are not considered in the results shown in Fig. 3.

A relatively new passive flow element, known as the inertance tube, utilizes the inertia of the oscillating flow to bring about a shift in the phase between the flow and the pressure [3]. The location of this inertance tube is shown in Fig. 4. For small pulse tube refrigerators where the mass flow in the inertance tube is small the phase shift may be only a few degrees. In order to achieve the optimum phase angle of flow lagging pressure by about 30° at the cold end means that the inertance tube will need to lag the flow at its inlet (junction with the pulse tube warm end) by about 60° to accommodate the change in phase through the pulse tube. Such a large negative phase for flow in the pulse tube component produces a large magnitude of flow for a given acoustic power flow. However, because the pulse tube is an open tube, large flows there do not contribute to large losses. However, a secondary flow known as acoustic streaming can occur inside the pulse tube that causes a loss. Tapering the pulse tube has been shown to reduce this loss [4]. The appropriate taper angle depends on the phase between the pressure and the flow. For the case of flow lagging pressure by about 50° at the pulse tube midpoint, the calculated taper becomes zero [4]. Coincidentally, such a phase angle is consistent with having the flow at the inertance tube inlet lag the pressure by about 60° , which we have already discussed is about the optimum phase to minimize the loss within the regenerator. Because a 60° phase shift is difficult to obtain in the inertance tube of small pulse tube refrigerators, we discuss in the rest of the paper how to use a simple, but relatively accurate, model of inertance tubes to find the unique diameter and length that gives the maximum phase shift.

INERTANCE TUBE MODEL

Transmission Line Analogy

The equations governing acoustic systems are the same form as those for AC electrical systems whenever pressure is substituted for voltage and volume flow substituted for current. The continuous nature of the inertance tube makes it analogous to an electrical transmission line. The electrical elements of resistance, inductance, and capacitance are substituted with the fluid elements of resistance, inertance, and compliance. Figure 5 represents a circuit diagram of a small differential element of the transmission line. The complex impedance of an electrical element is defined as

$$\text{(Electrical)} \quad Z = E / I, \quad (2)$$

where E is the voltage and I is the current. For fluid systems the impedance is

$$\text{(Fluid)} \quad Z = P / \dot{V} = \rho_0 P / \dot{m} = \rho_0 Z_m, \quad (3)$$

where P is the pressure, \dot{V} is the volume flow rate, and Z_m is the impedance to mass flow. We like the use of Z_m because mass flow is conserved, whereas volume flow is not. The resulting compliance of volume elements are like those used in the phasor diagrams of Figs. 1 and 2. For the fluid transmission line the resistance, inertance, and compliance per

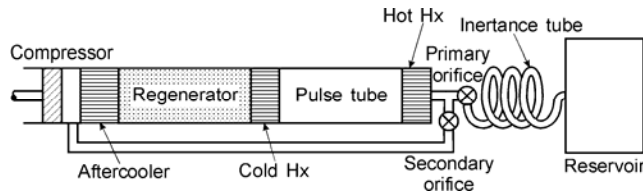


FIGURE 4. Schematic of a pulse tube refrigerator with an inertance tube and secondary orifice.

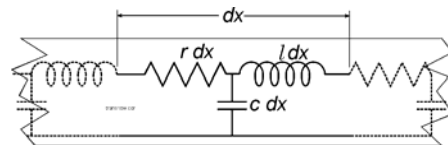


FIGURE 5. Equivalent circuit of a differential element of a transmission line.

unit length appropriate to Z_m are:

$$\text{(resistance/length)} \quad r(D) = (2/\pi) \left[\frac{32 f_r |\dot{m}|}{\pi^2 \rho_0 D^5} \right], \quad (4)$$

$$\text{(inertance/length)} \quad \ell(D) = 4/(\pi D^2), \quad (5)$$

$$\text{(compliance/length)} \quad c(D) = (\pi D^2)/(4\gamma RT_0), \quad (6)$$

where D is the tube inner diameter, f_r is the Fanning friction factor, and γ is the ratio of specific heats. The inclusion of γ in equation (6) implies an adiabatic process. For an isothermal process we make $\gamma = 1.0$ instead of 1.667. For some intermediate heat transfer process we can take γ to have any value between 1.0 and 1.667. The incorporation of the friction factor in equation (4) allows the use of this model in both the laminar and turbulent flow regions. We also take into account surface roughness in the calculation of the friction factor, but steady-state correlations for tubes are used rather than any complex oscillating flow correlation. There certainly is some question whether such a steady-state correlation is valid for oscillating flow, although our comparisons of the model with experiments in a later section show good agreement.

The reservoir of volume V_r at the end of the inertance tube introduces a compliant load on the end of the fluid transmission line of

$$C_r = V_r / (\gamma RT_r). \quad (7)$$

The impedance of this compliant load is

$$Z_r = 1/(i\omega C_r). \quad (8)$$

The complex impedance of a terminated transmission line of length L is given by [5]

$$Z_m(D, x) = Z_0(D) \left[\frac{Z_r + Z_0(D) \tanh[k(D)(L-x)]}{Z_0(D) + Z_r \tanh[k(D)(L-x)]} \right], \quad (9)$$

where the complex characteristic impedance is

$$Z_0(D) = \sqrt{\frac{r(D) + i\omega\ell(D)}{i\omega c(D)}}, \quad (10)$$

and the complex propagation function or wave number is

$$k(D) = \sqrt{[r(D) + i\omega\ell(D)]i\omega c(D)}. \quad (11)$$

The convention used here for the position x is that it is zero at the inlet to the inertance tube (pulse tube end) and increases to L at the reservoir end. The solution to equation (9) for $x = 0$ gives the amplitude $|Z_m|$ and phase θ_Z of the impedance at the inlet to the inertance tube.

The sign of θ_Z is opposite of that used earlier in this paper for θ since θ_Z indicates the phase by which P leads \dot{m} .

Comparison of Model with Experiment

Measurements of inertance tube impedance were carried out using a commercial linear compressor to provide the oscillating flow at the inlet to the inertance tube. Flow at the inlet was measured by a hot-wire anemometer and the flow at the reservoir end was determined by measuring the pressure in the reservoir and using the ideal gas equation for an adiabatic process

$$\dot{m}_r = \dot{P}V_r / \gamma RT_r. \quad (12)$$

The hot-wire anemometer was calibrated against \dot{m}_r when the inertance tube was replaced by a needle valve with small volume. The calibration did not appear to be affected by the

pressure amplitude, which could be varied by adjusting the valve setting. The experimental inertance tube was made rather long to provide a large compliance component that could be compared easily with the model prediction. The tube had an inner diameter of 1.58 mm and a length of 3.60 m. The reservoir volume was 77 cm³. For the measurements reported here the average pressure was 2.5 MPa, the frequency was 50 Hz, and the average temperature was about 300 K. With those conditions the thermal penetration depth δ_t in the helium gas was 0.219 mm, which yields a ratio $R/\delta_t = 3.60$, where R is the tube radius. With such a ratio we expect processes within the inertance tube to be somewhere between isothermal and adiabatic. Power into the compressor was varied in such a manner to provide pressure ratios at the inlet to the inertance tube in the range of 1.05 to 1.40. A comparison between the measured and calculated phase θ_z of the impedance is shown in Fig. 6. A comparison of the measured and calculated flow at the inlet is given in Fig. 7. Figure 8 compares the flow at the reservoir and Fig 9 compares the phase difference between the flows at each end. These figures show that there is good agreement between the model and experimental results. Most of the experimental results lie between the adiabatic and isothermal curves from the model, which would be expected for the tube diameter used in these experiments. Because of this good agreement between the model and experiments, we feel that design curves derived from the model would be useful.

OPTIMIZATION PROCEDURE

Selection of Input Parameters

In the design of pulse tube refrigerators the net refrigeration power is almost always a fixed input parameter. That refrigeration power is equal to the acoustic or PV power flow through the pulse tube minus the losses. These losses would normally be calculated in the design of the refrigerator. Thus, the acoustic power flow into the inertance tube is usually a fixed and known quantity. For a well-designed pulse tube refrigerator the net refrigeration power will be about 30% of the acoustic power in the pulse tube for a cold temperature of 80 K. The average pressure and pressure ratio are often fixed for the design, or they are optimized in some manner. The pressure amplitude then is usually considered a known input parameter. The design of the inertance tube must be such that for the given pressure amplitude at the inlet the desired acoustic power flow into the inertance tube occurs. Equation (1) gives the expression for the acoustic power flow, but includes the mass flow. From equation (3) we use the expression $|\dot{m}| = |P|/|Z_m|$ to substitute for \dot{m} in equation (1).

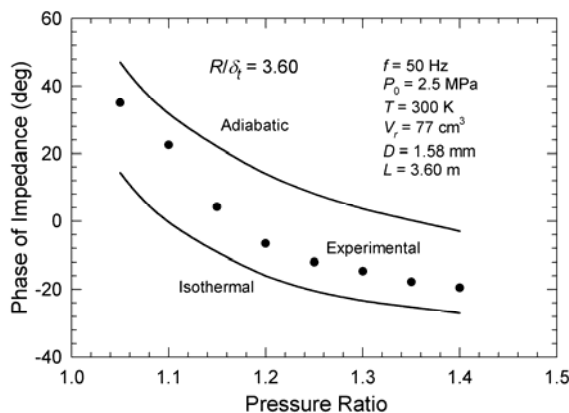


FIGURE 6. Measured and calculated phase of impedance of the inertance tube.

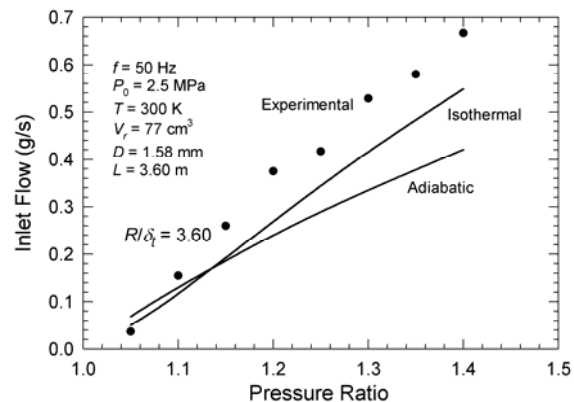


FIGURE 7. Measured and calculated mass flow rate at inlet to inertance tube.

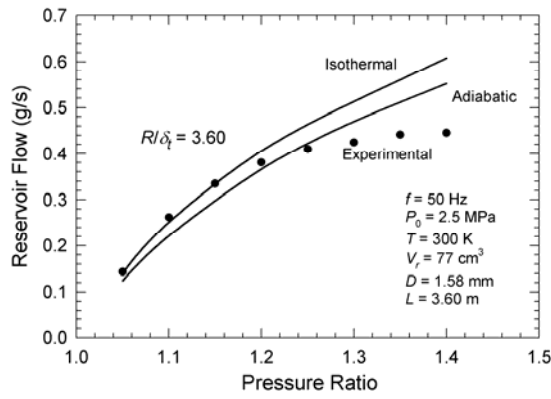


FIGURE 8. Measured and calculated mass flow rate at reservoir end of the inertance tube.

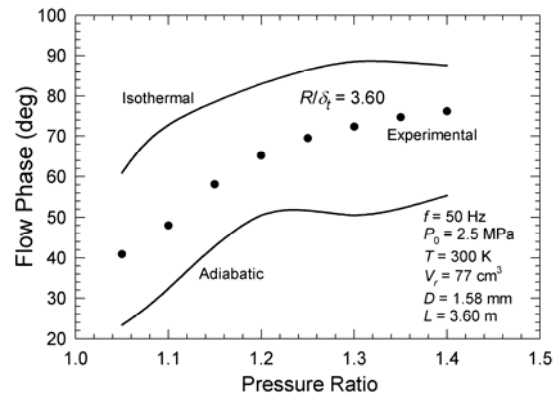


FIGURE 9. Measured and calculated phase between flows at each end of the inertance tube.

We then arrive at the equation

$$\frac{|Z_m|}{\cos \theta_Z} = \frac{(1/2)RT_0|P|^2}{P_0 \langle \dot{W} \rangle_t}, \quad (13)$$

which defines the locus of points where the complex Z_m allows for the specified acoustic power flow with the given pressure amplitude at the inlet.

Optimum geometry

The locus of points in the complex Z_m plane that satisfies equation (13) defines a locus of points in the D, L plane that give the desired Z_m . In general there are several curves in the D, L plane that represent solutions. Some have negative values of θ_Z , which we rule out, and others occur at longer lengths that represent higher multiples of $\lambda/2$, where λ is the acoustic wavelength. In the case of small acoustic power flow we search the locus of points in the D, L plane that provides the maximum positive value of θ_Z (negative θ). If this phase reaches about 60° , we then change our optimization procedure and now reduce the size of the reservoir volume to keep the phase shift at about 60° . However, here we only consider small acoustic power flows where we always maximize the phase shift.

OPTIMIZED DESIGN CURVES

Figure 10 shows the maximum phase shift θ_Z that any single inertance tube can provide according to the transmission line model discussed here. These results are for a frequency of 60 Hz, and average pressure of 2.5 MPa, an average temperature of 300 K, a surface roughness of $1 \mu\text{m}$, and an infinite reservoir volume. The effect of surface roughness is quite small. Curves are given for two pressure ratios and for both adiabatic and isothermal behavior in the inertance tube. Figure 11 gives the inside diameter of the optimized inertance tube, and Fig. 12 gives the corresponding length. We note that for small acoustic powers (less than about 5 W) the radius of the tube approaches the thermal penetration depth. In such a case the isothermal approximation may be more appropriate. Figure 13 shows the phase difference between flows at the two ends of the optimized inertance tube. This phase difference is caused by the compliance component in equation (6) of the inertance tube impedance. This large phase difference shows that the compliance component cannot be neglected.

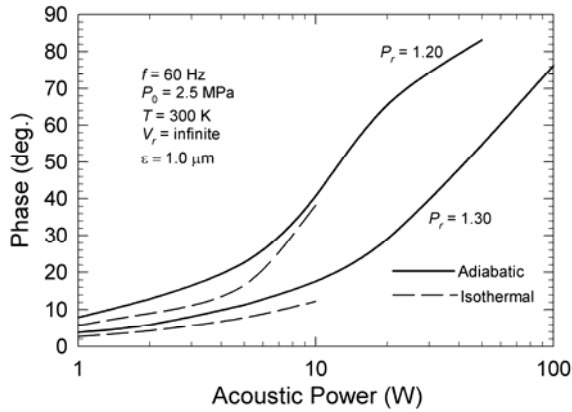


FIGURE 10. Maximum phase shift in inertance tubes optimized for a given acoustic power.

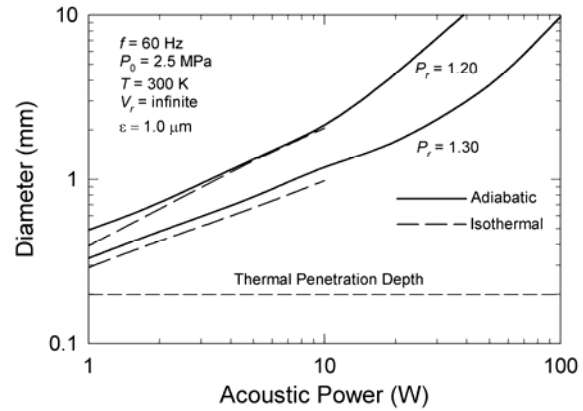


FIGURE 11. Inside diameter of optimized inertance tubes.

CONCLUSIONS

We have shown that the optimum phase between flow and pressure in any regenerative cycle is that with the flow and pressure in phase at about the midpoint of the regenerator. Such a phase minimizes regenerator losses. For a pulse tube refrigerator the gas volumes in the regenerator and in the pulse tube then require that the flow lag the pressure at the warm end of the pulse tube by about 60° in order to achieve the desired phase within the regenerator. An inertance tube will provide phase shifts in the right direction, but for low-power systems the magnitude of the phase shift is less than the optimum. As an aid to the designer we have shown how a simple transmission-line model of the inertance tube, which agrees well with experiments, can be used to find the optimum diameter and length of the inertance tube that gives the maximum phase shift for a given acoustic power.

REFERENCES

1. Radebaugh, R., "Pulse Tube Cryocoolers," in *Low Temperature and Cryogenic Refrigeration*, edited by S. Kakac, H.F. Smirnov, and M.R. Avelino, Kluwer Academic Publishers, Dordrecht, 2003, pp. 415-434.
2. Zhu, S., Wu, P., and Chen, Z., "Double Inlet Pulse Tube Refrigerators: An Important Improvement," *Cryogenics* **30**, 514 (1990).
3. Radebaugh, R., "Advances in Cryocoolers," in *Proc. 16th Int'l Cryogenic Eng. Conf./Int'l Cryogenic Materials Conf.*, Elsevier Science, Oxford (1997) pp. 33-44.
4. Olson, J.R., and Swift, G.W., "Acoustic Streaming in Pulse Tube Refrigerators: Tapered Pulse Tubes," *Cryogenics* **37**, 769-776 (1997).
5. Skilling, H.H., *Electric Transmission Lines*, McGraw-Hill, New York (1951).

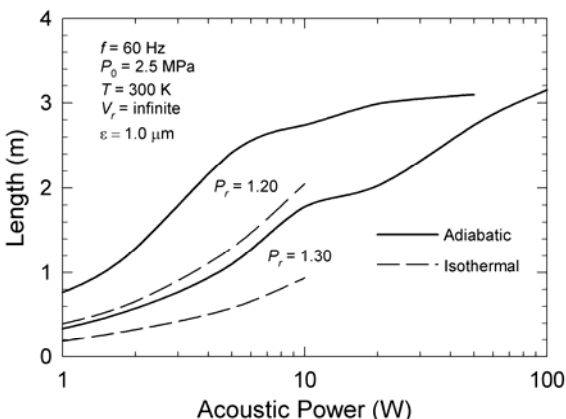


FIGURE 12. Length of optimized inertance tubes.

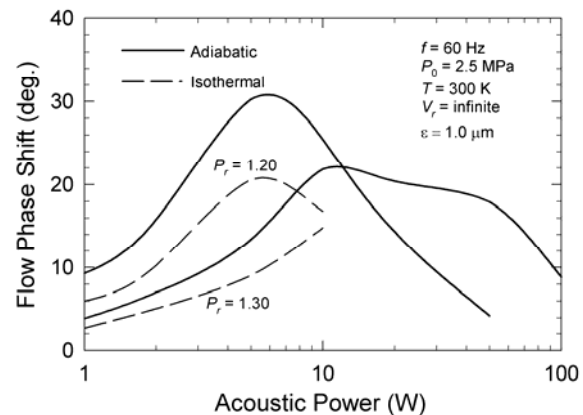


FIGURE 13. Phase shift between flows at each end of optimized inertance tubes.